Die Pharmazie

Pharmazie **2026**; 81(6): 52690
https://doi.org/10.31083/Pharmazie52690

Research Article

Guggulsterone Alleviates Atherosclerosis in ApoE$^{-/-}$ Mice by Modulating Lipid Metabolism and Inflammatory Responses Associated with Modulation of the *Srebp2*/*Hmgcr* Signaling Axis

Jialin Liang[1], Jingfang Zhang[1], Xun Huang[1], Jiahui Xu[1], Xinyu Luo[1], Jiaying Zhang[1], Cheng Huang[1], Kunhui He[1,*]

[1]The First Clinical Medical School, Changsha Medical University, 410219 Changsha, Hunan, China
*Correspondence: kunhui0406@163.com (Kunhui He)
Academic Editors: Mattia Mori and Walter E. Müller
Submitted: 8 April 2026 Revised: 7 May 2026 Accepted: 15 May 2026 Published: 25 June 2026

Abstract

Objective: Atherosclerosis (AS) is a chronic inflammatory vascular disease characterized by dysregulated lipid homeostasis and plaque formation. Consequently, there is an ongoing need for therapies with high efficacy and low toxicity. Thus, this study aimed to investigate the effects of guggulsterone (GS) on atherosclerotic plaques in mice and to elucidate the molecular mechanisms underlying the beneficial effects of GS in this pathological context. **Methods:** A total of 53 male ApoE$^{-/-}$ knockout mice were fed on a high-fat Western-type diet for 8 consecutive weeks to induce atherosclerotic lesions; three mice were randomly selected for model validation by serum lipid analysis and histopathological examination, and were excluded from subsequent grouping. The remaining 50 mice were randomly assigned to five groups (n = 10 per group): model group, low/medium/high-dose GS treatment groups (35/70/140 mg/kg GS, respectively), and an atorvastatin (AT) group (2.6 mg/kg). An additional 10 C57BL/6J mice served as the normal control group. After 8 weeks of intragastric treatment, serum lipid levels (Total cholesterol [TC], Triglycerides [TG], Low-density lipoprotein-cholesterol [LDL], High-density lipoprotein-cholesterol [HDL]) and a composite AS index were analyzed using standard biochemical methods. Serum nitric oxide (NO), monocyte chemoattractant protein-1 (MCP-1), interleukin-6 (IL-6), and prostacyclin (PGI2) levels were measured by enzyme-linked immunosorbent assay (ELISA). Aortic pathological changes were evaluated by hematoxylin and eosin staining, while monocyte/macrophage-specific monoclonal antibody 2 (MOMA-2) and α-smooth muscle actin (α-SMA) expression were evaluated by immunohistochemistry; Aortic Hmgcr and Srebp2 mRNA levels were quantified using reverse transcription quantitative polymerase chain reaction (RT-qPCR). Outcome assessments were conducted in a blinded manner. **Results:** Compared with the control group, the model group exhibited poorer general status, increased body weight, abnormal lipid levels, elevated levels of inflammatory factors, and typical aortic AS pathological changes (all $p < 0.05$), together with the upregulation of aortic *Srebp2* and *Hmgcr* mRNA levels (all $p < 0.05$). In contrast, mice in the medium- and high-dose GS groups and the AT treatment group exhibited improved general status, reduced body weight, normalized lipid levels and inflammatory factors, and ameliorated aortic pathological damage, along with the reversal of the molecular changes observed in AS model mice (all $p < 0.05$). Notably, high-dose GS exerted comparable or even superior regulatory effects versus AT on the levels of TC, TG, LDL, NO, PGI_2, IL-6 and MOMA-2. **Conclusion:** GS treatment reduces atherosclerotic plaque area and delays AS progression in mice, potentially through the regulation of *Srebp2*/*Hmgcr* mRNA expression, thereby improving lipid metabolism, inhibiting inflammatory responses, and enhancing autophagy.

Keywords: atherosclerosis; ApoE knockout mice; guggulsterone; lipid metabolism

1. Introduction

Atherosclerosis (AS) is a chronic pathological process characterized by persistent impairment of vascular wall structure and function, accompanied by lipid accumulation, intimal thickening, and sustained local inflammatory activation. With the progression of atherosclerotic lesions, plaque enlargement and instability may eventually result in vascular stenosis or occlusion, thereby contributing to the development of severe cardiovascular events [1,2]. Although the pathogenesis of AS is multifactorial and not yet fully elucidated, disorders of lipid metabolism and excessive inflammatory activation are generally considered major contributors to disease progression.

Previous studies have indicated that the *Srebp2/Hmgcr* signaling pathway is closely associated with the maintenance of metabolic balance and inflammatory regulation [3]. Several key molecules within this pathway are involved in the functional modulation of vascular smooth muscle cells and macrophages. Dysregulation of this signaling axis has been reported to facilitate abnormal proliferation and migration of vascular smooth muscle cells, reduce intracellular lipid clearance, and promote foam cell formation, thereby aggravating lipid metabolic disorders. Furthermore, activation of this pathway may stimulate downstream inflammatory signaling cascades, increase the production of pro-inflammatory mediators such as tumor necrosis

factor-α (TNF-α) and interleukin-6 (IL-6), and contribute to the progression of atherosclerotic lesions [4]. Previous evidence also suggests that targeting the Srebp2/Hmgcr signaling pathway may alleviate lipid metabolism abnormalities and inflammatory responses, thereby slowing the progression of AS [5].

However, it is important to note that the pathogenesis of AS involves a complex regulatory network of multiple signaling pathways. In addition to *Srebp2/Hmgcr*, other pathways such as NF-κB signaling and oxidative stress-related mechanisms also play critical roles in vascular inflammation and endothelial dysfunction. Recent studies have demonstrated that guggulsterone (GS) can inhibit NF-κB nuclear translocation and reduce reactive oxygen species (ROS) generation, thereby alleviating 7-ketocholesterol-induced vascular endothelial injury [6]. These findings suggest that the protective effects of GS on the cardiovascular system are mediated through the modulation of multiple pathways rather than a single signaling axis.

GS is a resin component extracted from the traditional Chinese medicine *Commiphora myrrha*, and is the predominant material basis for the pharmacological effects of this medicine. Its functions include promoting blood circulation to relieve pain, reducing swelling, and promoting granulation, and in addition to pronounced antioxidant, anti-inflammatory, lipid-lowering, microcirculation-improving, and blood stasis-alleviating effects [7]. Studies have reported that GS treatment significantly improves lipid metabolism in model animals, as evidenced by the decreased levels of key indicators such as Total cholesterol (TC), Triglycerides (TG), and Low-density lipoprotein-cholesterol (LDL), suggesting its regulatory effect on abnormal lipid metabolism [8]. Moreover, as a selective antagonist of farnesoid X receptor (FXR), GS exerts anti-inflammatory and lipid-regulating pharmacological effects through mechanisms that may be related to the regulation of lipid metabolism and vascular endothelial protection pathways [9]. Recent evidence has further clarified the molecular basis of these effects [10]. A comprehensive review published in 2025 systematically demonstrated that GS antagonizes FXR to promote cholesterol efflux and suppress inflammatory signaling, thereby contributing to the improvement of lipid metabolism and vascular inflammation. In addition, consistent with its anti-inflammatory and endothelial protective roles, GS has been shown to attenuate vascular endothelial injury by inhibiting NF-κB activation and reducing oxidative stress [11].

In pharmacological and preclinical animal studies, GS has been shown to potentially mitigate core pathological processes driving AS progression [12]. However, there has been relatively little research focused on its direct effect on the stability of AS plaques or the underlying molecular regulatory mechanisms, emphasizing a need to clarify the signaling pathways and key targets of GS treatment. As such, the present study was developed to provide experimental support for the utility of GS as an intervention for AS prevention or management by identifying its regulatory effects on gene expression in this disease, with a particular focus on the *Srebp2*/*Hmgcr* mRNA levels.

2. Materials and Methods

2.1 Experimental Animals

Fifty-three 8-week-old SPF male ApoE$^{-/-}$ mice (18–21 g) and ten C57BL/6J mice were purchased from Changzhou Cavens Laboratory Animal Co., Ltd. (License No.: SCXK (Su) 2021-0013). All mice were housed in a specific pathogen-free animal room with good ventilation, a temperature of 24 ± 1 ℃, humidity of 45%–65%, and a 12 h light/dark cycle, with free access to food and water. This study was approved by the Animal Ethics Committee of Changsha Medical University (No. 2023-014). All anesthesia and euthanasia procedures were performed in strict accordance with the ARRIVE guidelines and the animal welfare regulations approved by the Animal Ethics Committee of Changsha Medical University, to minimize the pain and distress of experimental animals. The sample size (n = 10 per group) was determined based on previous studies using the same ApoE$^{-/-}$ mouse atherosclerosis model, in which groups of 10 mice were sufficient to detect significant differences in key outcomes [13].

2.2 Drugs and Reagents

Guggulsterone (purity ≥98%, Batch No.: 230526) was purchased from Shanghai Yiji Industrial Co., Ltd., Shanghai, China. A triglyceride assay kit (Cat. No.:S03027), cholesterol assay kit (Cat. No.:S03042), and High-density lipoprotein-cholesterol (HDL) assay kit (Cat. No.:S03025) were obtained from Shenzhen Rayto Life Sciences Co., Ltd., Shenzhen, China. An interleukin-6 (IL-6) Enzyme-linked immunosorbent assay (ELISA) kit (Cat. No.:GEM0001), a monocyte chemoattractant protein-1 (MCP-1) ELISA kit (Cat. No.:GEM0017), an α-smooth muscle actin (α-SMA) antibody (Cat. No.:GB111364), and hydrochloric acid (Cat. No.:10011028) were purchased from China National Pharmaceutical Group Chemical Reagent Co., Ltd. PBS (Cat. No.:G0002), universal tissue fixative (Cat. No.:G1101), bovine serum albumin (BSA) (Cat. No.:GC305010), normal rabbit serum (Cat. No.:G1209), a hematoxylin-eosin (H&E) staining kit (Cat. No.:G1004), hematoxylin differentiation solution (Cat. No.:G1039), hematoxylin bluing solution (Cat. No.:G1040), HRP-conjugated goat anti-rabbit IgG (Cat. No.:GB23303), TBST (Cat. No.:G2150-1L), 0.45 μm PVDF membranes (Cat. No.:WGPVDF45), a BCA protein quantification kit (Cat. No.:G2026), a general ECL chemiluminescence kit (Cat. No.:G2014-50ML), a 50× protease inhibitor cocktail (Cat. No.:G2006-250UL), phosphatase inhibitors (Cat. No.:G2007-1ML), and OCT embedding

medium (Cat. No.:G6059-110ML) were all from Wuhan Servicebio Technology Co., Ltd., Wuhan, China.

2.3 Instruments

This study utilized a decolorizing shaker, vortex mixer, and high-speed tissue grinder from Wuhan Servicebio Technology Co., Ltd., Wuhan, China; an electronic balance from Mettler-Toledo Instruments (Shanghai) Co., Ltd.; a cryostat microtome from Thermo Fisher Scientific Inc.; a microplate reader from BioTek Instruments, Inc., USA; a desktop high-speed refrigerated centrifuge from Dragon Lab Instruments (Beijing) Co., Ltd.; an automatic biochemical analyzer from Shenzhen Rayto Life Sciences Co., Ltd., Shenzhen, China; an electric constant temperature water bath from Shanghai Jinghong Experimental Equipment Co., Ltd.; a microwave oven from Galanz Microwave Appliances Co., Ltd.; and a microscope from Nikon Instruments Inc.

2.4 Model Establishment and Grouping

After adaptive feeding, C57BL/6J mice were used as the normal control group, while the remaining ApoE$^{-/-}$ mice were fed a high-fat diet to establish an AS model [14]. During the modeling period, the general status of the mice was continuously observed. Of the 53 utilized ApoE$^{-/-}$ mice, 3 were randomly selected for model validation via serum lipid analysis and histopathological examination, and were not included in subsequent grouping. After successful model establishment, the remaining ApoE$^{-/-}$ mice were randomly divided into 5 groups using a random number table, including a model group, low-dose GS group (35 mg/kg), medium-dose GS group (70 mg/kg), high-dose GS group (140 mg/kg), and AT group (2.6 mg/kg), with 10 mice per group. All drugs were administered once daily by gavage for 8 consecutive weeks. Outcome assessments were conducted in a blinded manner.

2.5 Body Weight Measurement

The body weight of mice in each group was monitored during the experiment, with measurements being recorded once per week at a fixed time. A body weight change curve was plotted to evaluate the effects of different treatments on overall growth status.

2.6 Sample Collection

After the 8-week intervention, mice were fasted for 12 h with free access to water. Blood samples were collected via the orbital venous plexus under inhalation anesthesia with 3% isoflurane (RWD Life Science, China). Following blood collection, mice were humanely sacrificed by intraperitoneal administration of 1% sodium pentobarbital (100 mg/kg body weight, Merck, Germany), strictly adhering to the institutional humane endpoint criteria and animal welfare protocols. Death was confirmed by the permanent cessation of heartbeat and breathing, and the aortic tissues were quickly isolated on ice. The isolated tissues were divided and treated according to the subsequent experimental requirements, with partial tissues fixed in 4% paraformaldehyde for pathological analysis, and the rest being snap-frozen in liquid nitrogen and stored at –80 °C for subsequent molecular biology detection.

2.7 Detection of Serum TC, TG, LDL, HDL Levels and AS Index Calculation

Serum levels of TC, TG, LDL, and HDL were detected using an automated biochemical analyzer in strict accordance with the provided instructions. The AS index, which was used to comprehensively evaluate the degree of dyslipidemia, was calculated according to the following formula [15]: AS index = (TC - HDL) / HDL.

2.8 ELISAs

Frozen serum samples were used to detect the expression levels of nitric oxide (NO), prostacyclin (PGI2), MCP-1, and IL-6 using appropriate ELISA kits in accordance with the provided directions. All plates were read using a microplate reader.

2.9 Evaluation of Aortic Pathology

Aortic tissues were fixed with paraformaldehyde, then dehydrated and cleared using standard methods, embedded in paraffin, and cut into sections for H&E staining and observation of the morphological structure of vascular walls and related pathological changes under a microscope.

2.10 Immunohistochemistry

Immunohistochemical staining was used to detect the expression of monocyte/macrophage-specific monoclonal antibody 2 (MOMA-2) and α-SMA in aortic tissues. Positive staining area was analyzed in a semi-quantitative manner in ImageJ (Version 1.53t, National Institutes of Health, Bethesda, MD, USA).

2.11 Reverse transcription quantitative polymerase chain reaction (RT-qPCR)

Total RNA was extracted from aortic tissues and reverse-transcribed into cDNA. RT-qPCR was used to detect the expression of *Hmgcr* and *Srebp2* at the mRNA level, using *Gapdh* expression as a normalization control. All primers used for this study are shown in Table 1.

2.12 Statistical Analysis

SPSS 26.0 (IBM Corp., Armonk, NY, USA) was used for all data analysis. Continuous data were expressed as the mean ± standard deviation ($\overline{x} \pm s$). Body weight data were analyzed using repeated-measures ANOVA to evaluate the effects of Group, Time, and the Group × Time interaction. Other multi-group comparisons (such as serum lipids, inflammatory cytokines, and mRNA expression levels) were performed using one-way analysis of variance

Table 1. Primer sequences.

Primer name	Sequence	Number of base pairs	Product length/bp
Hmgcr	F: ACAGCGGAGCAGGCTAAGGT	20	239
	R: TTTGAGGTCACGACGGGAGA	20	
Srebp2	F: CAAGAAGAAGGCAGGCGACC	20	103
	R: CACAAATCCCACAGAGTCCACA	22	
Gapdh	F: CCTCGTCCCGTAGACAAAATG	21	133
	R: TGAGGTCAATGAAGGGGTCGT	21	

(ANOVA), followed by Tukey's post-hoc test for pairwise comparisons. $p < 0.05$ was considered significant.

3. Results

3.1 General Status of Mice in Each Group

During the entire experimental period, mice in the control group exhibited good general health status, with high fur luster, frequent activity, sensitive responses, and a stable mental state. Mice in the model group exhibited obvious abnormalities, including dull fur, reduced activity, and lethargy, indicating successful model establishment. Compared with the model group, mice in each treatment group showed varying degrees of improvement in fur color, activity, and mental state after intervention.

3.2 GS Attenuates High-Fat Diet-Induced Body Weight Gain in ApoE$^{-/-}$ Mice

Before modeling, there were no significant differences in general status or body weight among all experimental groups ($p \geq 0.05$). During the high-fat diet intervention, the body weight of mice in all groups showed a gradual increasing trend, with no significant difference among groups ($p \geq 0.05$). By Week 8, following the high-fat diet induction, the body weight of mice in the model group and all treatment groups showed a significant and consistent increase compared with the control group ($p < 0.05$, Table 2), confirming the successful establishment of the obesity model prior to drug intervention. Following the commencement of GS or AT treatment, the body weight in the treatment groups exhibited a progressive decrease and was significantly lower than that in the model group during the subsequent observation weeks ($p < 0.05$), as evidenced by the repeated-measures ANOVA results (Fig. 1, Table 2).

3.3 Serum TC, TG, LDL, HDL, and AS Index Analyses

Compared with the control group, serum levels of TC, TG, and LDL in the model group were significantly increased, while HDL levels were significantly decreased, and the AS index was significantly elevated (all $p < 0.05$), which collectively verified the successful induction of atherosclerotic lesions in our experimental mouse model. Compared with the model group, serum TC, TG, and LDL levels in mice treated with different doses of GS showed a downward trend with GS dose, while HDL levels rose gradually, and the AS index was significantly reduced in all treatment groups (all $p < 0.05$). The strongest effects were observed in response to medium- and high-dose GS treatment, with evidence of dose-dependence. The positive control AT treatment group exhibited beneficial effects similar to those in the high-dose GS group (Fig. 2).

3.4 Serum NO, PGI2, MCP-1, and IL-6 Levels

Compared with the control group, the serum levels of NO and PGI2 in the model group were decreased by 61.54% and 80.85%, respectively, while the levels of MCP-1 and IL-6 were increased by 281.83% and 89.92% (all $p < 0.05$), indicating a significant enhancement of the inflammatory response. Compared with the model group, the PGI2 level in the low-dose GS group was increased by 31.51%, while MCP-1 and IL-6 levels were decreased by 3.39% and 10.02% (all $p < 0.05$), respectively, and NO levels were not significantly affected ($p \geq 0.05$). The NO levels in the medium/high-dose GS groups and the AT group were increased by 60.00%, 100.00%, and 120.00% relative to the model group, respectively, while PGI2 levels were increased by 105.47%, 269.95%, and 314.34%, MCP-1 levels were reduced by 25.72%, 25.75%, and 36.24%, and IL-6 levels were reduced by 25.51%, 34.25%, and 40.49% (all $p < 0.05$). Notably, the high-dose GS group exhibited therapeutic effects comparable to the AT group, with no significant differences observed between them ($p \geq 0.05$, Fig. 3).

3.5 Aortic Pathological Changes

The aortic intima of mice in the control group was intact with smooth vascular walls and no obvious lipid deposition. The aortic intima of mice in the model group was significantly thickened with massive lipid deposition, and foam cell aggregation and plaque formation were observed. Compared with the model group, all GS-treated groups and the AT group showed decreased aortic lipid deposition and reduced plaque area, with the high-dose GS group and AT group exhibiting stronger ameliorative effects (Fig. 4).

3.6 Aortic MOMA-2 and α-SMA Protein Expression

A significant increase in positive MOMA-2 and α-SMA staining area was observed in the aortas of mice in the model group ($p < 0.05$), suggesting obvious smooth muscle cell proliferation and inflammatory infiltration. In response to GS or AT intervention, MOMA-2 expression

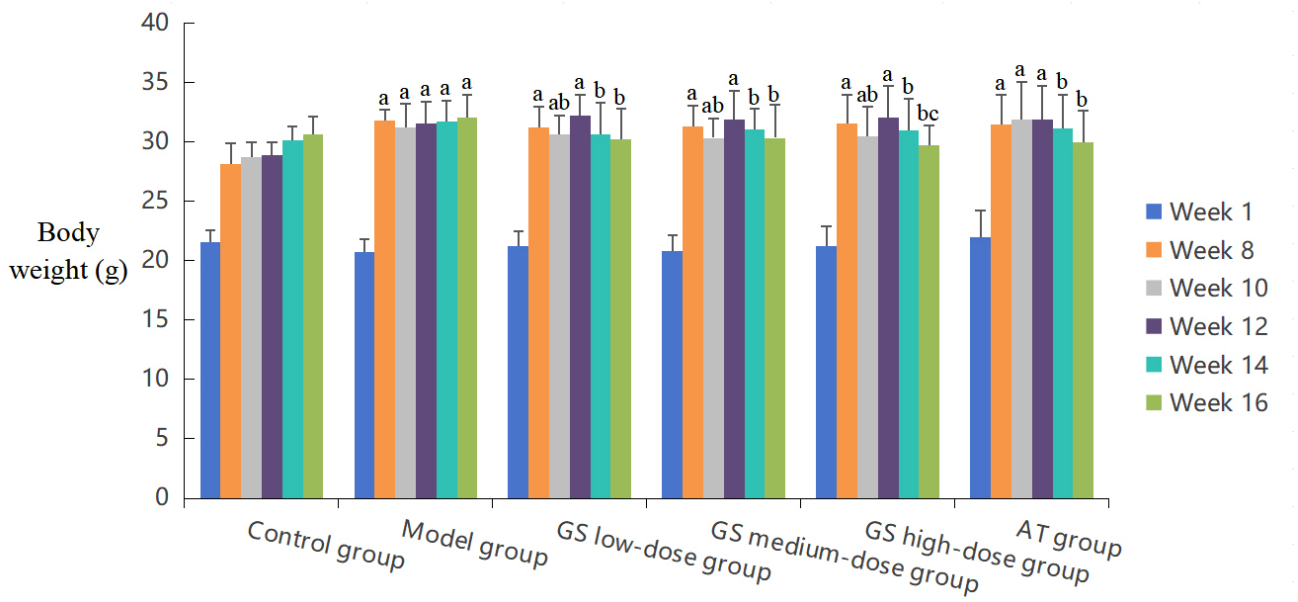

Fig. 1. Body weight measurements among different groups of mice (n = 10 per group). Dynamic changes in body weight were measured in all six experimental groups (Control, Model, low-dose guggulsterone [GS], medium-dose GS, high-dose GS, and atorvastatin [AT] positive control groups) at Weeks 1, 8, 10, 12, 14, and 16. Results are presented as mean ± SD. Statistical significance was determined using repeated-measures ANOVA followed by Tukey's post-hoc test: a, compared with the control group ($p < 0.05$); b, compared with the AS model group ($p < 0.05$); c, compared with the GS low-dose group. SD, Standard Deviation.

Table 2. Body weight comparisons among different groups of mice.

Groups	n	Week 1	Week 8	Week 10	Week 12	Week 14	Week 16
Control group	10	21.53 ± 1.07	28.17 ± 1.13	28.68 ± 1.30	28.85 ± 1.36	30.10 ± 1.72	30.63 ± 2.27
Model group	10	20.69 ± 1.68	31.82 ± 0.89[a]	31.25 ± 1.73[a]	31.51 ± 1.78[a]	31.70 ± 2.46[a]	32.06 ± 2.51[a]
GS low-dose group	10	21.21 ± 1.29	31.24 ± 1.92[a]	30.59 ± 1.62[a,b]	32.23 ± 1.59[a]	30.63 ± 2.52[b]	30.21 ± 3.18[b]
GS medium-dose group	10	20.78 ± 1.11	31.30 ± 1.84[a]	30.34 ± 1.75[a,b]	31.87 ± 2.42[a]	31.03 ± 2.68[b]	30.34 ± 2.84[b]
GS high-dose group	10	21.19 ± 1.17	31.54 ± 1.74[a]	30.44 ± 2.67[a,b]	32.01 ± 1.75[a]	30.95 ± 2.66[b]	29.75 ± 2.82[b,c]
AT group	10	21.96 ± 1.52	31.45 ± 1.91[a]	31.84 ± 2.62[a]	31.86 ± 2.76[a]	31.17 ± 1.59[b]	29.98 ± 2.65[b]

Note: Data are presented as mean ± SD (n = 10). Statistical analysis was performed using repeated-measures ANOVA. Repeated-measures ANOVA revealed significant main effects of Group and Time, as well as a significant Group × Time interaction (all $p < 0.05$). a, compared with the control group ($p < 0.05$); b, compared with the AS model group ($p < 0.05$); c, compared with the GS low-dose group ($p < 0.05$).

was significantly downregulated, while α-SMA expression was markedly increased in a dose-dependent manner across the low-dose, medium-dose, and high-dose GS groups ($p < 0.05$), indicating that inflammatory infiltration was alleviated and plaque stability was enhanced. These results confirm that both interventions can effectively inhibit vascular wall inflammation and ameliorate associated structural abnormalities (Figs. 5,6).

3.7 Aortic Hmgcr and Srebp2 mRNA Expression

Compared with the control group, the mRNA levels of *Hmgcr* and *Srebp2* in the aortas of mice in the model group were increased by 71.00% and 35.00%, respectively (all $p < 0.05$). Compared with the model group, *Hmgcr* expression at the mRNA level in the low/medium/high-dose GS groups and the AT group was decreased by 21.64%, 37.43%, 56.14% and 51.46%, while the corresponding expression of *Srebp2* was decreased by 4.43%, 11.11%, 21.48% and 44.43% (all $p < 0.05$). Notably, high-dose GS treatment demonstrated inhibitory effects on Hmgcr and Srebp2 expression comparable to those of the AT group ($p \geq 0.05$, Fig. 7).

4. Discussion

AS is a chronic vascular disease caused by lipid deposition in the arterial wall, inflammation, and vascular endothelial dysfunction, with the core drivers of pathogenesis being arterial intimal damage and abnormal lipid metabolism leading to vascular stenosis or occlusion, ultimately inducing cardiovascular and cerebrovascular dis-

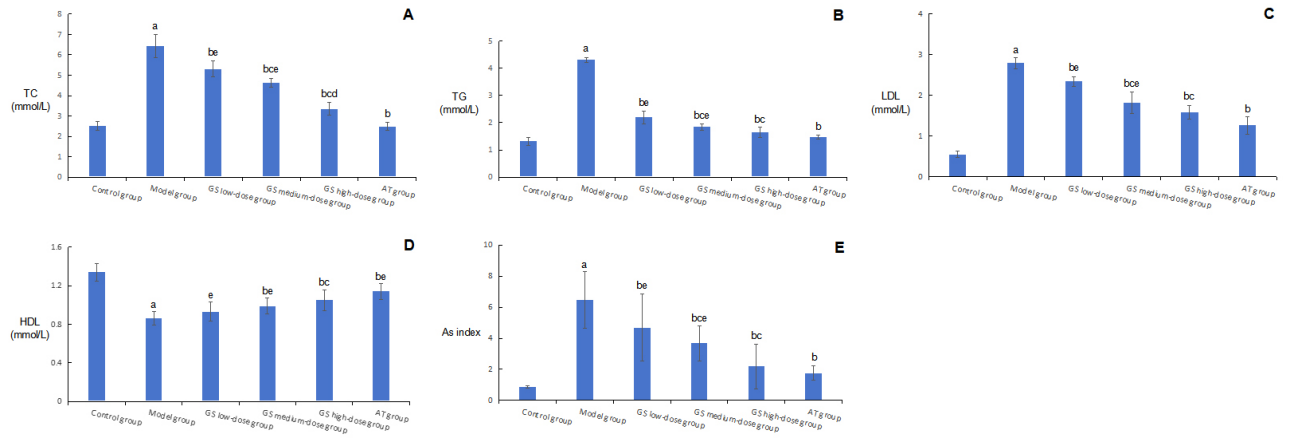

Fig. 2. Comparison of serum total cholesterol (TC), triglycerides (TG), low-density lipoprotein-cholesterol (LDL), high-density lipoprotein-cholesterol (HDL), and AS index levels among different groups of mice. (A–E) Changes in serum TC, TG, LDL, HDL, and AS index among different experimental groups. GS treatment improved lipid metabolism and reduced the AS index in a dose-related manner compared with the model group. Results are presented as mean ± SD. Statistical significance was indicated as follows: a, compared with the control group ($p < 0.05$); b, compared with the AS model group ($p < 0.05$); c, compared with the GS low-dose group ($p < 0.05$); d, compared with the GS medium-dose group ($p < 0.05$); and e, compared with the GS high-dose group ($p < 0.05$).

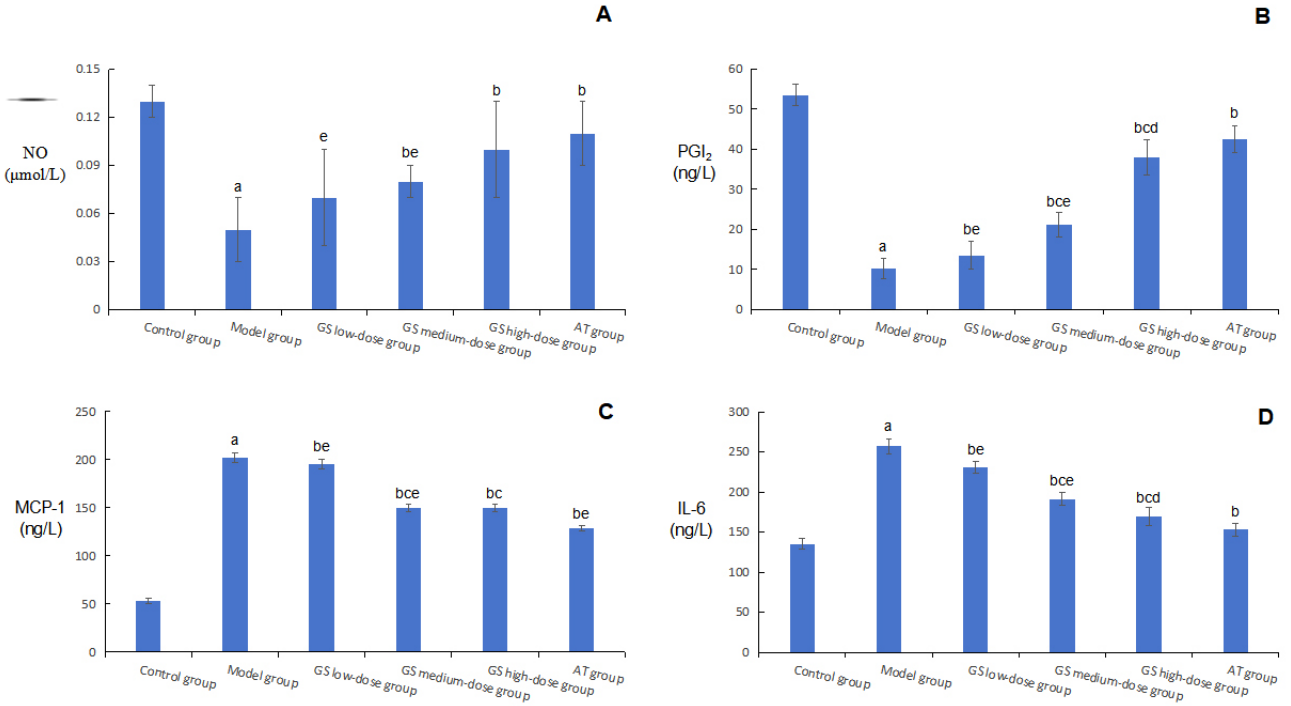

Fig. 3. Comparison of serum NO, MCP-1, IL-6, and PGI2 levels among different groups of mice. Bar graphs demonstrating endothelial protective and anti-inflammatory activity of guggulsterone (GS) and atorvastatin (AT) across six experimental cohorts: normal control group, atherosclerotic model group, low-dose GS group, medium-dose GS group, high-dose GS group, and AT positive control group. (A) Serum nitric oxide (NO) levels. (B) Serum prostacyclin (PGI2) levels. (C) Serum monocyte chemoattractant protein-1 (MCP-1) levels. (D) Serum interleukin-6 (IL-6) levels. Results are presented as mean ± SD. Statistical significance was indicated as follows: a, compared with the control group ($p < 0.05$); b, compared with the AS model group ($p < 0.05$); c, compared with the GS low-dose group ($p < 0.05$); d, compared with the GS medium-dose group ($p < 0.05$); and e, compared with the GS high-dose group ($p < 0.05$).

ease [15]. Although statins can improve this disease to some extent in the clinic, long-term medication can give rise to adverse reactions [16], emphasizing the value of exploring safe and effective alternative interventional measures.

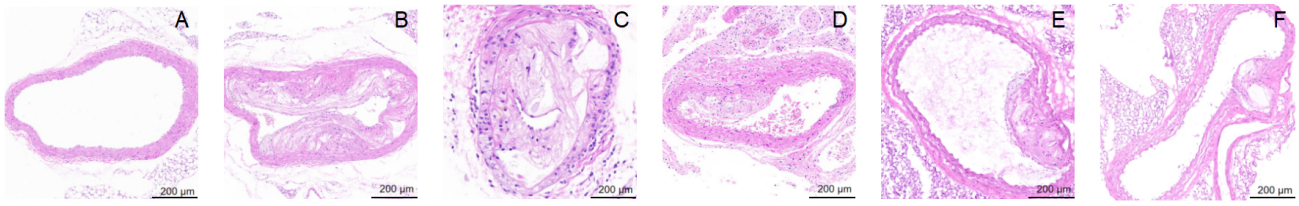

Fig. 4. Hematoxylin-eosin (H&E) staining of the aorta in different groups of mice. Micrographs illustrating aortic morphological and pathological changes across six experimental cohorts, with a scale bar of 200 μm for all images. (A) Normal control group. (B) Atherosclerotic model group. (C) GS low-dose group. (D) GS medium-dose group. (E) GS high-dose group. (F) AT positive control group.

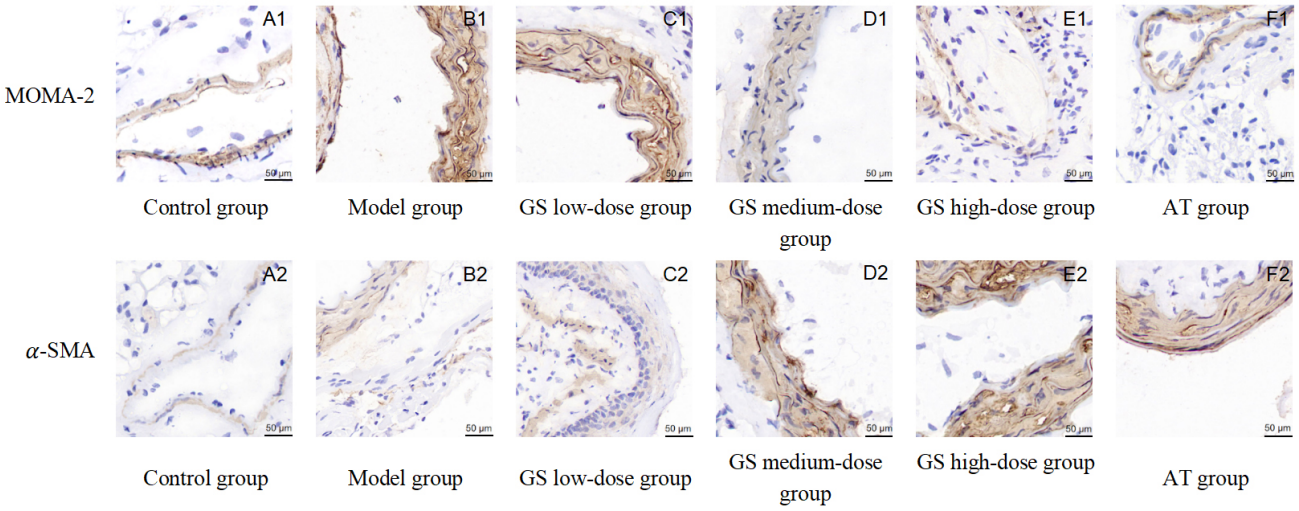

Fig. 5. Results of immunohistochemical staining of the aorta in different groups of mice. Representative images showing monocyte/macrophage-specific monoclonal antibody 2 (MOMA-2) and α-smooth muscle actin (α-SMA) staining in aortic tissues of mice from the control, model, GS-treated, and AT groups. GS treatment reduced inflammatory infiltration and promoted the accumulation of α-SMA-positive smooth muscle cells compared with the model group. (A1–F1): MOMA-2 staining (A1: control group, B1: model group, C1: GS low-dose group, D1: GS medium-dose group, E1: GS high-dose group, F1: AT-treated group); (A2–F2): α-SMA staining (A2: control group, B2: model group, C2: GS low-dose group, D2: GS medium-dose group, E2: GS high-dose group, F2: AT-treated group). GS treatment reduced inflammatory infiltration and abnormal vascular smooth muscle changes compared with the model group. Scale bar = 50 μm.

The dysregulation of lipid metabolism is a key pathological driver of the progression of AS lesions. Abnormal increases in TC, TG, and LDL levels, coupled with lower HDL levels, directly lead to lipid deposition in the vascular endothelium, promoting foam cell formation and atherosclerotic plaque progression. As an important indicator for evaluating lipid metabolism disorder and AS risk, the AS index reflects the elevated risk of disease occurrence [17]. In addition, *Hmgcr* and *Srebp2* are key regulators of cholesterol synthesis, and their overexpression enhances endogenous cholesterol production in addition to aggravating lipid accumulation.

In the present study, ApoE$^{-/-}$ mice fed a high-fat diet were used as a widely accepted model to simulate the pathological characteristics of human AS [18]. In these experimental animals, GS or AT treatment improved lipid metabolism, as evidenced by decreased TC, TG, and LDL levels, increased HDL levels, and a reduced AS index. Histopathological analysis further indicated that GS or AT reduced aortic pathological lesion severity, while also associated with *Srebp2/Hmgcr* mRNA expression changes. Taken together, these findings suggest that GS treatment is associated with improvements in lipid metabolism-related indicators. These results are generally consistent with previous reports [19].

The inflammatory response is a central driver of the initiation and progression of AS, involving inflammatory cell recruitment, cytokine release, and vascular dysfunction [20]. MCP-1 plays a key role in recruiting monocytes to vascular lesions, where they differentiate into macrophages,

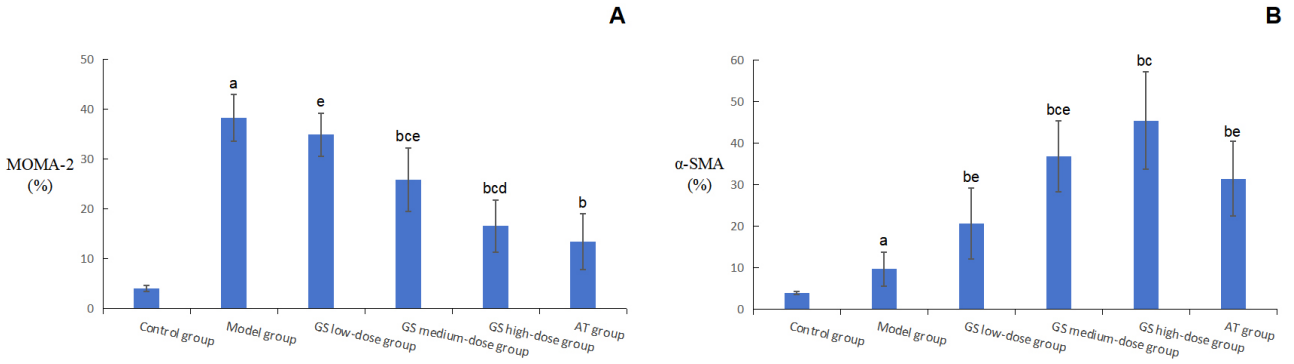

Fig. 6. Comparison of the percentage of MOMA-2 and α-SMA positive area in the aortas of mice in different experimental groups. Quantification of the immunohistochemical staining in Fig. 5 was performed. (A) Percentage of positive expression area of the macrophage-specific marker MOMA-2. (B) Percentage of positive expression area of the vascular smooth muscle cell marker α-SMA. Results are presented as mean ± SD. Statistical significance was indicated as follows: a, compared with the control group ($p < 0.05$); b, compared with the AS model group ($p < 0.05$); c, compared with the GS low-dose group ($p < 0.05$); d, compared with the GS medium-dose group ($p < 0.05$); and e, compared with the GS high-dose group ($p < 0.05$).

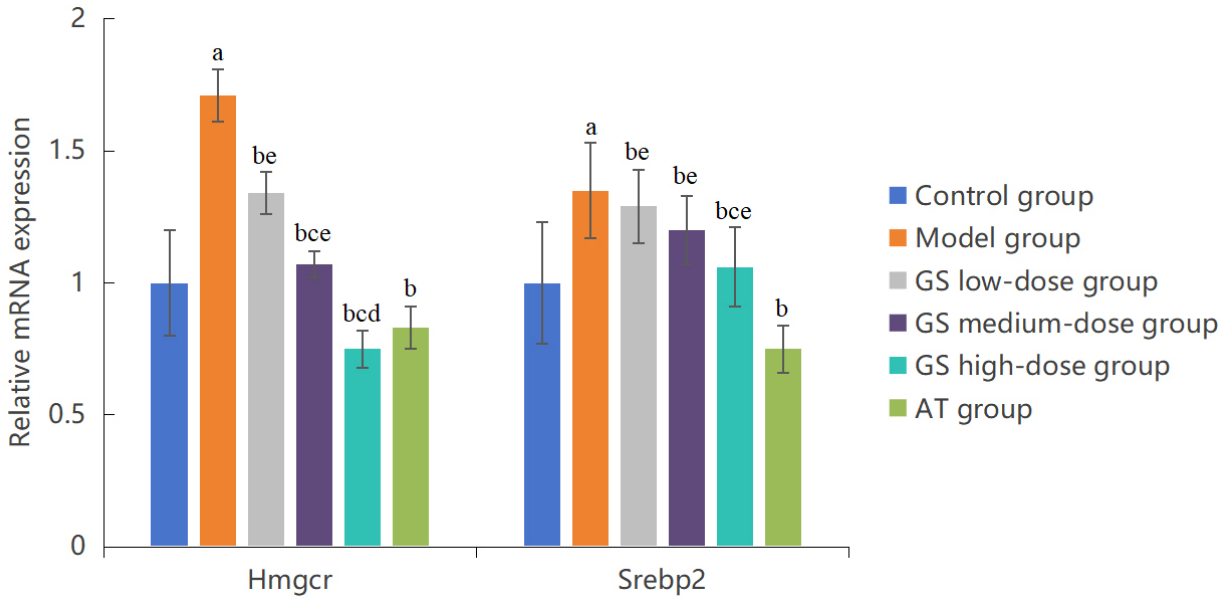

Fig. 7. Comparison of the relative mRNA expression levels of *Hmgcr* and *Srebp2* in the aortas of mice in different experimental groups (n = 10). Reverse transcription quantitative polymerase chain reaction (RT-qPCR) was used to analyze the mRNA expression of Hmgcr and Srebp2, two key regulators of cholesterol and lipid metabolism. Results are presented as mean ± SD. Statistical significance was indicated as follows: a, compared with the control group ($p < 0.05$); b, compared with the AS model group ($p < 0.05$); c, compared with the GS low-dose group ($p < 0.05$); d, compared with the GS medium-dose group ($p < 0.05$); and e, compared with the GS high-dose group ($p < 0.05$).

as reflected by MOMA-2 expression [21]. IL-6 further exacerbates endothelial injury, while α-SMA is closely associated with vascular smooth muscle cell activation and plaque stability [22]. NO and PGI2 are important endothelial-derived protective factors that regulate vascular tone and inhibit thrombosis and inflammation [23,24]. Excessive inflammatory responses can reduce NO and PGI2 levels, establishing a vicious cycle that aggravates vascular dysfunction [25].

The results of the present study revealed that GS or AT treatment helped mitigate the imbalance between proinflammatory and protective factors in AS model mice, as indicated by decreased MCP-1 and IL-6 levels together with increased NO and PGI2 levels. In addition, reduced MOMA-2 expression and increased α-SMA expression suggested the alleviation of macrophage infiltration and improved vascular remodeling. Associated with *Srebp2/Hmgcr* mRNA expression changes was also ob-

served in the GS and AT groups. These findings suggest that GS treatment may be associated with the modulation of inflammatory responses and lipid metabolism-related pathways. However, it should be noted that such changes do not establish a direct mechanistic link between these findings, and further studies are required to clarify the underlying molecular pathways. However, these findings are generally consistent with previous reports [26]. In the present study, the regulatory role of GS was primarily verified at the mRNA level. Further investigations involving protein expression analysis and functional rescue experiments are needed to fully substantiate the mediation of the Srebp2/Hmgcr signaling pathway.

One prior study reported that GS may aggravate atherosclerotic lesions in ApoE$^{-/-}$ mice [27]. The discrepancy between that study and the present findings may be attributable to differences in experimental conditions, such as dosage, treatment duration, dietary composition, or model variability. This suggests that the effects of GS on AS may be context-dependent and require further investigation.

In addition, accumulating evidence indicates that the cardiovascular protective effects of GS involve multiple signaling pathways [28]. For example, GS has been reported to attenuate endothelial injury by inhibiting NF-κB nuclear translocation and reducing reactive oxygen species (ROS) generation. Furthermore, GS acts as an FXR antagonist, promoting cholesterol efflux and exerting anti-inflammatory effects, as summarized in a recent review [29]. These findings suggest that the effects of GS are likely mediated through a complex, multi-pathway regulatory network rather than a single signaling axis.

In conclusion, GS intervention can improve lipid metabolism, alleviate inflammatory response, and effectively inhibit the progression of atherosclerotic lesions in ApoE$^{-/-}$ mice. These effects are associated with alterations in lipid metabolism and inflammatory pathways, although a definitive causal relationship cannot be established based on the current data. This study provides experimental evidence supporting the potential value of GS as an approach to AS treatment. However, given the multi-target nature of traditional Chinese medicine, further studies are required to elucidate the precise molecular mechanisms underlying its effects and to validate these findings.

5. Limitations

Despite demonstrating the anti-atherosclerotic effects of GS in ApoE$^{-/-}$ mice, several limitations of this study should be acknowledged. First, GS was administered by oral gavage, a route associated with relatively low bioavailability. Previous studies have reported that the absolute oral bioavailability of Z-GS in rats is approximately 42.9%, indicating a substantial first-pass effect. Limited systemic exposure may therefore underestimate its pharmacological efficacy. In addition, oral administration is influenced by gastrointestinal conditions and metabolic variability, which may contribute to experimental heterogeneity. Second, the precise mechanism of action remains incompletely defined. Although our findings highlight the regulatory effects of GS on Srebp2 and Hmgcr, these observations were primarily limited to the mRNA level. The absence of protein expression analysis (e.g., Western blot) and pathway-specific rescue experiments means that the definitive mediating role of the *Srebp2/Hmgcr* signaling pathway requires further substantiation. Additionally, GS is also a known FXR antagonist, and its effects may result from direct modulation of intracellular signaling proteins or indirect receptor-mediated mechanisms. The lack of pathway-specific intervention precludes definitive conclusions regarding causality. Third, the potential differences between Z- and E-isomers were not addressed. GS consists of both stereoisomers, which differ in pharmacokinetics and biological activity. The use of mixed isomers may obscure isomer-specific effects, particularly given their rapid clearance and short half-lives observed *in vivo*. Fourth, the evaluation of atherosclerotic lesions in this study was primarily based on H&E staining. While H&E staining provides essential morphological information regarding intimal thickening and foam cell aggregation, more specific staining methods, such as Oil Red O for lipid deposition or Masson's trichrome for collagen content, would provide more comprehensive evidence for plaque characterization. Nonetheless, the pathological assessment in the present study was supplemented by quantitative serum lipid profiles and immunohistochemical analysis of MOMA-2 and α-SMA, which collectively support the ameliorative effects of GS on AS lesions. Furthermore, the study is limited by a relatively small sample size and the use of a single animal model. Although ApoE$^{-/-}$ mice are widely used, they do not fully replicate human AS. Validation in additional models (e.g., LDL receptor-deficient mice or large animal models) is warranted. Finally, no translational or clinical validation was performed. Therefore, the relevance of these findings to human atherosclerosis remains to be established. Future studies should address these limitations, including optimization of drug delivery strategies [30] and further mechanistic investigations.

6. Conclusion

In this study, GS significantly lowered TC, TG, and LDL-C, increased HDL-C, and markedly reduced aortic pathological lesion severity, while this process was associated with *Srebp2/Hmgcr* mRNA expression changes. GS suppressed MCP-1 and IL-6 production while enhancing NO and PGI2 levels, reducing MOMA-2 expression, and increasing α-SMA levels. These results suggest that GS may attenuate AS, but such effects are associative observations that do not establish causality. This study is limited by the lack of mechanistic insight, dose-response analyses, and safety assessment. Future studies should attempt to validate the underlying mechanisms, optimize dosing, and evaluate the efficacy and safety of GS in different animal models

and clinical settings. In summary, GS shows potential as a therapeutic agent in AS, but caution is warranted.

Availability of Data and Materials

The data used and analyzed during the current study are available from the corresponding author upon reasonable request.

Author Contributions

Conceptualization: JL; KH; Methodology: JL; JZ; XH; Investigation: JL; JZ; XH; JX;CH; Data Curation: JL; Formal Analysis: JL; JZ; XL; Writing – Original Draft: JL; Writing – Review & Editing: JL; KH; XL; JZ; Supervision: KH; Funding Acquisition: JL. All authors contributed to editorial changes in the manuscript. All authors have read and agreed to the published version of the manuscript. All authors have participated sufficiently in the work and agreed to be accountable for all aspects of the work.

Ethics Approval and Consent to Participate

All animal experiments were conducted in strict accordance with the Guide for the Care and Use of Laboratory Animals (National Institutes of Health, USA) and approved by the Animal Ethics Committee of Changsha Medical University (Approval No. 2023-014). All efforts were made to minimize animal suffering, reduce the number of animals used, and adhere to the ARRIVE guidelines to ensure the scientificity and ethicality of the experiments.

Acknowledgment

We would like to express our sincere gratitude to the Education Department of Hunan Province and all other funding institutions for their generous support.

We would like to thank Changsha Medical University for providing the experimental platform and research conditions for this study. We also express our sincere thanks to all colleagues in the laboratory for their selfless help and technical support during the experiments, as well as all members of the research team for their full cooperation in experimental operation and data collation.

We are also grateful to all the experts and scholars who put forward valuable comments and suggestions during the manuscript review process.

We extend our heartfelt thanks to our families and friends for their constant understanding, support and encouragement during the research. The successful completion of this study could not have been achieved without the great help of every teacher, colleague, relative and friend, and we hereby express our most heartfelt gratitude to all of them!

Funding

This work was supported by the Educational Department of Hunan Province through the College Students' Innovation and Entrepreneurship Training Program (Xiangjiaotong [2023] No.237-4068).

Conflicts of Interest

The authors declare no conflicts of interest.

Supplementary Material

Supplementary material associated with this article can be found, in the online version, at https://doi.org/10.31083/Pharmazie52690.

References

[1] Poznyak AV, Kashirskikh DA, Postnov AY, Popov MA, Sukhorukov VN, Orekhov AN. Sialic acid as the potential link between lipid metabolism and inflammation in the pathogenesis of atherosclerosis. Brazilian Journal of Medical and Biological Research = Revista Brasileira De Pesquisas Medicas E Biologicas. 2023; 56: e12972. https://doi.org/10.1590/1414-431X2023e12972

[2] Lavillegrand JR, Al-Rifai R, Thietart S, Guyon T, Vandestienne M, Cohen R, et al. Alternating high-fat diet enhances atherosclerosis by neutrophil reprogramming. Nature. 2024; 634: 447–456. https://doi.org/10.1038/s41586-024-07693-6

[3] Bauer R, Brüne B, Schmid T. Cholesterol metabolism in the regulation of inflammatory responses. Frontiers in Pharmacology. 2023; 14: 1121819. https://doi.org/10.3389/fphar.2023.1121819

[4] Feng X, Du M, Li S, Zhang Y, Ding J, Wang J, et al. Hydroxysafflor yellow A regulates lymphangiogenesis and inflammation via the inhibition of PI3K on regulating AKT/mTOR and NF-κB pathway in macrophages to reduce atherosclerosis in ApoE-/- mice. Phytomedicine : International Journal of Phytotherapy and Phytopharmacology. 2023; 112: 154684. https://doi.org/10.1016/j.phymed.2023.154684

[5] Ozkan-Nikitaras T, Grzesik DJ, Romano LEL, Chapple JP, King PJ, Shoulders CC. N-SREBP2 Provides a Mechanism for Dynamic Control of Cellular Cholesterol Homeostasis. Cells. 2024; 13: 1255. https://doi.org/10.3390/cells13151255

[6] Sabarathinam S, Ganamurali N. Targeting 7-ketocholesterol-induced oxidative stress and inflammation: Guggulsterone as a novel vascular protectant. The Journal of Steroid Biochemistry and Molecular Biology. 2025; 254: 106846. https://doi.org/10.1016/j.jsbmb.2025.106846

[7] Guo QQ, Liu MN, Liu TL. Research progress on pharmacological effects of guggulsterone. Acta Chinese Medicine and Pharmacology. 2022; 50: 115–119. https://doi.org/10.19664/j.cnki.1002-2392.220096 (In Chinese)

[8] Dudekula JB, Koilpillai J, Narayanasamy D. Guggulsterone phytosomes: A novel approach to alleviate hyperlipidemia in high-fat diet-fed rats. Journal of Herbmed Pharmacology. 2024; 13: 80–89. https://doi.org/10.34172/jhp.2024.48111

[9] Adarsh Krishna TP, Ajeesh Krishna TP, Edachery B, Antony Ceasar S. Guggulsterone - a potent bioactive phytosteroid: synthesis, structural modification, and its improved bioactivities. RSC medicinal chemistry. 2023; 15: 55–69. https://doi.org/10.1039/d3md00432e

[10] Sabarathinam S, Ganamurali N. Steroidal scaffold dichotomy: pathogenic role of 7-ketocholesterol versus protective FXR-antagonistic actions of guggulsterone in metabolic regulation.

Steroids. 2025; 223: 109691. https://doi.org/10.1016/j.steroids.2025.109691

[11] Sabarathinam S, Aggarwal BB. Guggulsterone inhibits NF-kappaB and IkappaBalpha kinase activation, suppresses expression of anti-apoptotic gene products, and enhances apoptosis. The Journal of biological chemistry. 2004; 279: 47148–47158. https://doi.org/10.1074/jbc.M408093200

[12] Deng R. Therapeutic effects of guggul and its constituent guggulsterone: cardiovascular benefits. Cardiovascular Drug Reviews. 2007; 25: 375–390. https://doi.org/10.1111/j.1527-3466.2007.00023.x

[13] Ying T, Wu L, Lan T, Wei Z, Hu D, Ke Y, et al. Adropin inhibits the progression of atherosclerosis in ApoE-/-/Enho-/- mice by regulating endothelial-to-mesenchymal transition. Cell Death Discovery. 2023; 9: 402. https://doi.org/10.1038/s41420-023-01697-3

[14] Wang L, Fang TF, Bao JF, Lin SD, Wang M, Guo BL, et al. Effect and mechanism of Dendrobium officinale on atherosclerosis in ApoE-/- mice. Prev Treat Cardio Cerebrovasc Dis. 2024; 24: 13–16.

[15] Xu TS, Zhang YY, Chai WJ, Yin JY, Wang LL, Liu B, et al. Allicin ameliorates atherosclerosis in ApoE-/- mice by regulating TLR4/MyD88/NF-κB pathway. Chin Herb Med. 2024; 55: 6636–6644.

[16] Zeng W, Deng H, Luo Y, Zhong S, Huang M, Tomlinson B. Advances in statin adverse reactions and the potential mechanisms: A systematic review. Journal of Advanced Research. 2025; 76: 781–797. https://doi.org/10.1016/j.jare.2024.12.020

[17] Zhang H, Long X, Niu G, Shi W, Zhao Z, Feng D, et al. Genetic insights into lipid traits and atherosclerosis risk: a Mendelian randomization and polygenic risk score analysis. International Journal of Surgery (London, England). 2025; 111: 6802–6815. https://doi.org/10.1097/JS9.0000000000002869

[18] Luo SW, Luo QY, Nie J, Li L, Wei JY, Chen HQ, et al. Analysis of animal models of atherosclerosis based on clinical syndrome characteristics of traditional Chinese and western medicine. Chinese Journal of Comparative Medicine. 2024; 34: 115–127. https://doi.org/10.3969/j.issn.1671-7856.2024.08.014 (In Chinese)

[19] Chae HS, Kim HJ, Ko HJ, Lee CH, Choi YH, Chin YW. Transcriptome Analysis Illuminates a Hub Role of SREBP2 in Cholesterol Metabolism by α-Mangostin. ACS Omega. 2020; 5: 31126–31136. https://doi.org/10.1021/acsomega.0c04282

[20] Kong P, Cui ZY, Huang XF, Zhang DD, Guo RJ, Han M. Inflammation and atherosclerosis: signaling pathways and therapeutic intervention. Signal Transduction and Targeted Therapy. 2022; 7: 131. https://doi.org/10.1038/s41392-022-00955-7

[21] Han LP, Wang TH, Cao LB, Yang HY. Effect and mechanism of ligustrazine on atherosclerotic plaques in ApoE-/- mice. Chinese Journal of Arteriosclerosis. 2025; 33: 673–682. https://doi.org/10.20039/j.cnki.1007-3949.2025.08.004 (In Chinese)

[22] Li M, Wu L, Wen Y, Wang A, Zhou X, Ren L, et al. Dysregulated cholesterol uptake and efflux of bone marrow-derived α-SMA+ macrophages contribute to atherosclerotic plaque formation. Cellular and Molecular Life Sciences : CMLS. 2025; 82: 134. https://doi.org/10.1007/s00018-025-05655-3

[23] Shaito A, Aramouni K, Assaf R, Parenti A, Orekhov A, Yazbi AE, et al. Oxidative Stress-Induced Endothelial Dysfunction in Cardiovascular Diseases. Frontiers in Bioscience (Landmark Edition). 2022; 27: 105. https://doi.org/10.31083/j.fbl2703105

[24] Wautier JL, Wautier MP. Pro- and Anti-Inflammatory Prostaglandins and Cytokines in Humans: A Mini Review. International Journal of Molecular Sciences. 2023; 24: 9647. https://doi.org/10.3390/ijms24119647

[25] Takenoshita Y, Tokito A, Jougasaki M. Inhibitory Effects of Eicosapentaenoic Acid on Vascular Endothelial Growth Factor-Induced Monocyte Chemoattractant Protein-1, Interleukin-6, and Interleukin-8 in Human Vascular Endothelial Cells. International Journal of Molecular Sciences. 2024; 25: 2749. https://doi.org/10.3390/ijms25052749

[26] Ganamurali N, Devarajan M, Sabarathinam S. Guggulsterone, a Classical Lipid-Lowering Phytosteroidal FXR Antagonist, as a Modulator of Lipid Signaling and Metabolic Reprogramming in Cancer. Lipids. 2026; 61: 279–284. https://doi.org/10.1002/lipd.70030

[27] Leiva A, Contreras-Duarte S, Amigo L, Sepúlveda E, Boric M, Quiñones V, et al. Gugulipid causes hypercholesterolemia leading to endothelial dysfunction, increased atherosclerosis, and premature death by ischemic heart disease in male mice. PLOS ONE. 2017; 12: e0184280. https://doi.org/10.1371/journal.pone.0184280

[28] Yang X, Ge C, Song J, Hu D, Tan Q, Xu R, et al. Unlocking the hidden health benefits of guggulsterone isolated from ancient spices: a comprehensive review. Chinese journal of natural medicines. 2026; 24: 145–155. https://doi.org/10.1016/S1875-5364(26)61086-2

[29] Sabarathinam S, Ganamurali N. Steroidal scaffold dichotomy: pathogenic role of 7-ketocholesterol versus protective FXR-antagonistic actions of guggulsterone in metabolic regulation. Steroids. 2025; 223: 109691. https://doi.org/10.1016/j.steroids.2025.109691

[30] Dudekula JB, Koilpillai J, Narayanasamy D. Guggulsterone phytosomes: a novel approach to alleviate hyperlipidemia in high-fat diet-fed rats. Journal of Herbmed Pharmacology. 2024; 13: 80–89. https://doi.org/10.34172/jhp.2024.48111